Available online at www.sciencedirect.com
SCIENCE DIRECT®
Journal of Nuclear Materials 325 (2004) 195–201
journal of nuclear materials
www.elsevier.com/locate/jnucmat

Immobilization of interstitial loops by substitutional alloy and transmutation atoms in irradiated metals

G.A. Cottrell *, S.L. Dudarev, R.A. Forrest

Culham Science Centre, EURATOM/UKAEA Fusion Association, Abingdon, Oxon OX143DB, UK

Received 13 June 2003; accepted 3 December 2003

Abstract

Small platelike clusters of self-interstitial atoms (SIAs) in irradiated metals are extremely mobile. This mobility can be greatly reduced by foreign atoms. Where the plates are large enough to form edge dislocation loops, their immobilization is analysed as a solid solution hardening. The misfitting substitutional solute atoms can significantly reduce the mobility of small SIA loops when in the central cores of their edge dislocation lines. An activation energy is required to unpin a loop from such atoms and this – unlike in conventional solid solution hardening – remains finite even with no applied stress driving the dislocation. In dilute solutions break-away occurs by the thermally activated escape from single atom obstacles on the loops. Application to a proposed fusion power plant alloy (EUROFER 97) shows that the W alloy atoms provide the most severe immobilization, although Mn atoms produced by transmutation run a close second. The contribution of Cr is evaluated.

1. Introduction

Molecular dynamics computer modeling of irradiation cascades and their evolution has revealed the importance of the motion of small interstitial loops [1–5]. The ('one-dimensional') mobility of such defects is large in perfect lattices and this feature has consequences for microstructural evolution. The mobility of individual self-interstitial atoms (SIAs) has of course been known since early studies of irradiation damage in which, for example, copper irradiated at 4 K and then annealed at progressively higher temperatures shows a first recovery (stage I) at about 40 K, attributed to the migrations of mobile SIAs. More recently, Ehrhart and Averback [6] have used diffuse X-ray scattering to examine small SIA loops in irradiated nickel and to show, by their coarsening, that they are mobile at temperatures below 300 K.

When SIA loops are very small, fewer than about 100 interstitials, they are best regarded as flat clusters of crowdions, all aligned along the same close packed direction, and their mobility is a result of the individual mobilities of the component crowdions in this direction [7]. The better model for a loop larger than this, which is the case that we shall consider below, is that of an edge dislocation ring, in which case the mobility is due to the glissile character of this dislocation in the direction of its Burgers vector.

Experimental demonstrations of the high mobility of SIAs and their loops have generally been made on pure metals, whereas a practical material to be used in, for example, a fusion power plant will usually contain alloy and impurity atoms, as well as gaining additional foreign atoms by transmutation. Such atoms are expected to reduce the SIA mobility and thus significantly change the evolution of microstructure and properties during a service lifetime. If the foreign atoms misfit the lattice there are two possibilities. When they occupy substitutional atomic sites, the atoms will cause a dilatational strain which interacts usually weakly with defects. However, if the impurity in the bcc lattice is at an

* Corresponding author. Tel.: +44-1235 466 426; fax: +44-1235 466 435.
E-mail address: geoff.cottrell@ukaea.org.uk (G.A. Cottrell).

0022-3115/$ - see front matter © 2004 UKAEA. Published by Elsevier B.V. All rights reserved.
doi:10.1016/j.jnucmat.2003.12.001

interstitial site (half way along a cell-edge) then the distortion is tetragonal and there are very strong interactions with appropriate defects. Only very small atoms (e.g. H, He, C, N) go preferentially into such sites and thereby become capable of exerting such strong pinning effects. While H and He are usually important transmutation products, their high mobilities at typical power plant operational temperatures will generally lead them away into distributions other than atomic solid solution.

In the following we shall be concerned, not with these, but with the effects of larger foreign atoms in dilute substitutional solution. They are expected to be randomly distributed and, because of their low diffusivity at typical power plant operational temperatures, to remain so during operational service. There is experimental evidence that such atoms reduce the mobility of SIAs and their loops [1–5]. For example, the presence of a trace of a solute such as Ag, Au or Cd, typically <1 at.%, in Cu eliminates stage I recovery (≈40 K) on annealing after irradiation at 4 K, and replaces it [8] by a new recovery stage, II, at ≈125 K. The elimination is attributed to the pinning and immobilization of the SIAs by the solute atoms and the recovery at higher temperature to the thermal release of these trapped SIAs. Again, the study of SIA loops in irradiated Ni showed that the coarsening of these at 300 K was suppressed by the presence of 1 at.% of Si which was considered to have immobilized the uncoarsened loops [6].

2. Theory

2.1. Solid solution hardening

When the SIA cluster, in the form of a disc, becomes large enough to be representable as a loop of edge dislocation which is mobile in the direction of its Burgers vector, the obstruction to its motion by foreign atoms in dispersed solid solution becomes identical with the corresponding local interactions of a full-length glide dislocation; and these interactions are the basis of the standard theory of solid solution hardening. The general theory of such hardening has been developed through various stages and most recently by Zaiser [9] whose method and notation we shall largely follow.

Through their strain fields, an edge dislocation loop and a misfitting solute atom interact at long range, but only weakly. Moreover, the algebraic sum of the forces on the loop, from a surrounding field of such atoms, averages to zero, in which case the field exerts no obstruction to the motion of the ring. We thus ignore it and consider only short range interactions, in particular the interaction when the atom is in the central core of the dislocation. We approximate Zaiser's expression for the interaction, $-\widehat{U}f(\mathbf{r})$, where $f(\mathbf{r})$ is a non-dimensional function of the range w of the interaction (with $f(0) = 1$), by a step-function interaction which attains its full value U_0 $(= -\widehat{U}f(0))$ when the atom is in the core; and is otherwise zero. We define the boundaries of this core as the two atomic sites on the compressed side of the core, which sit on the two sides of the terminal atom of the edge half-plane; and the two sites which face them on the expanded side of the core; four sites in all, i.e. A, B, C, D in Fig. 1. Thus we take $w = b$, where b = Burgers vector length ($b^3 \approx$ atomic volume).

The basic idea in the theory of solid solution hardening is that the dislocation line sits in a field of randomly arranged energy hills and valleys, which represent interactions with the solute atoms. The line attempts to take advantage of this by following a curved path which wanders along the valleys. In such a position it is pinned by the solutes, in the sense that its interaction energy has to increase, as a result of its passing over a hill-top into the next valley, in order to move forward. The adoption of the curved valley path involves, however, a lengthening of the line, compared with the shortest distance between its end points, and so is opposed by the line energy, represented by the line tension T, commonly taken to be $\frac{1}{2}\mu b^2$ where μ is the elastic shear modulus. Each path of local equilibrium is thus a compromise between opposite tendencies. Since a section has to move a distance of at least w, to cross the hill-top from one valley to the next, fine-scaled curves are disallowed because they involve excessive increase in line energy. Thus, for a given deflection w, there is a minimum length of segment, ξ_L, the Larkin–Labusch length [10], given by

$$\xi_L \approx \left(\frac{Tw}{2U_0 c^{1/2}}\right)^{2/3}, \tag{1}$$

where c is the volume density of the solutes. The $c^{1/2}$ factor occurs because the field of hills and valleys is brought about by the fluctuations δc in c, i.e. $\delta c = (c/V)^{1/2}$ in a volume V. Energy hills of size ξ_L have characteristic height

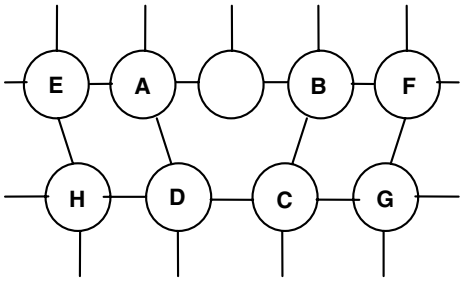

Fig. 1. The four core boundary atoms in an edge dislocation; A and B on the compressed side; C and D on the expanded one. When the dislocation moves one step to the right, atoms F and G move into the boundary, i.e. F → B, G → C; and those in A and D move out of it, to positions E and H.

$$E_{\mathrm{L}} = \left(\frac{T}{2}\right)^{1/3} w^{4/3} U_0^{2/3} c^{1/3}. \tag{2}$$

Since, when a segment of length ξ_{L} bends to a deflection w, this gain E_{L} is balanced by the increase of line energy, there is no net energy change so that hills on the scale ξ_{L} are unable to pin the dislocation, when this requires bending it to this deflection w. But the random solution provides hills on all scales and for one of size X ($> \xi_{\mathrm{L}}$) the interaction energy gain E ($> E_{\mathrm{L}}$), for an optimum deflection $Y(X)$, can exceed the increase of the line energy, so that the fully curved valley from there has lower energy than the straight line directly across the hill-tops. Hence on such large scales the dislocation can always be pinned by the fluctuations and needs an external energy supply to move over them. Zaiser gives

$$Y(X) = w\left(\frac{X}{\xi_{\mathrm{L}}}\right)^{2/3} \tag{3}$$

and for the pinning energy

$$E(X) \approx E_{\mathrm{L}}\left(\frac{X}{\xi_{\mathrm{L}}}\right)^{1/3}. \tag{4}$$

There are two sources of external energy, thermal fluctuations and work done by an applied shear stress, τ, which drives the dislocation towards the hill-top. The critical value τ_{c}, is that where the work done by τ is sufficient to supply all the solute pinning energy over a length ξ_{L}, i.e.

$$\tau_{\mathrm{c}} \approx \frac{U^{4/3} c^{2/3}}{T^{1/3} w^{1/3} b}. \tag{5}$$

For stresses, τ, less than this a thermal activation energy,

$$E_M(\tau) = cE_{\mathrm{L}}\left(\frac{\tau_{\mathrm{c}}}{\tau}\right)^{1/4}, \tag{6}$$

is required to reach the top of the barrier. After such an activation, the dislocation is equally likely to fall back into its original valley, or forward into the next one in which case the activation produces a successful jump.

2.2. Dilute solutions

The above analysis assumes that the solute atoms are sufficiently abundant for the hills and the valleys to be representable as a continuous field. But this may not be possible in dilute solutions. We need to consider how many solute atoms are encountered in a length ξ_{L} of the dislocation, i.e. how many on average change their energy by $\pm U_0$ as the length ξ_{L} moves by one atomic spacing b, which we are taking as the interaction distance w. In the cross-section of this edge dislocation (Fig. 1) there are four sites where the movement b can bring about this energy change, two just ahead of the core in the glide direction, one of them (F) on the compressed side and one (G) on the expanded side, which become part of the core as a result of the movement; and two more correspondingly (A and D), on the trailing side which get left behind as the dislocation moves forward. Hence the dislocation has four 'encounter' sites per atom of its length; i.e. $4\xi_{\mathrm{L}}/b$ sites in length ξ_{L}. The volume concentration c of solute corresponds to an atomic concentration cb^3. Hence the number N of encountered solute atoms in the length ξ_{L} is

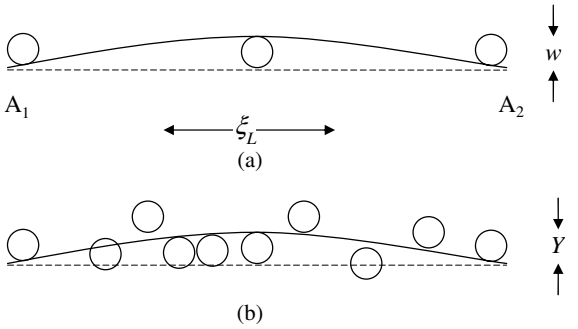

Fig. 2. A dislocation loop (opened up straight, by splitting at A_1, A_2) pinned by solute atoms: (a) $N < 1$, and (b) $N > 1$.

$$N = 4cb^2\xi_{\mathrm{L}}. \tag{7}$$

There are then two cases: $N > 1$ and especially $N \gg 1$, which is that of the theory above, and $N < 1$. An example we shall consider later shows that both of these are possible. These two cases are illustrated in Fig. 2.

The case $N < 1$ is that where the average distance between individual encountered solute atoms, along the line, is greater than the length ξ_{L}. Pinning by single atoms is then possible, since the bowing w can be accommodated in lengths $X > \xi_{\mathrm{L}}$, with a corresponding reduction of the extra line energy. In the limit of sufficiently small N the extra line energy becomes negligible, in comparison with the single atom interaction energy; and so we can take the pinning energy simply as $\approx U_0$ for each encountered solute atom, in this limit.

3. Application

3.1. SIA dislocation loop

The present problem differs from that of general solid solution hardening in two respects. First, the line length X is limited to the finite and short perimeter of the SIA loop. Second, in the problem considered here, which concerns the effects of irradiation, there is

Table 1
Fractional concentrations of principal atoms (transmutants >100 appm) after irradiation of EUROFER 97 in the first wall (zone 12) for 10 000 days in a fusion power plant

Element	Typical initial composition (C_i in appm) of EUROFER 97 [adapted from Ref. [15]]	Post-irradiation composition: (i.e. original atomic concentration + transmutation creation – transmutation destruction (appm)	Mean distance, $\langle d \rangle$ (nm), between species atoms assuming uniform distribution	Atomic volumes of impurities in the pure solid form ($\times 10^{-29}$ m^3)
Cr	90 000	94 018	0.5	1.21
W	10 800	5742	1.27	1.59
Mn	4800	55 610	0.6	1.47
V	2000	11 018	1.03	1.40
Ta	1500	1499		
C	1100	857		
Si	450	297		
Ni	200	311	3.38	1.03
N	210	153		
Al	90	105		
Ti	60	1063	2.23	1.76
Co	60	173	4.1	1.11
S	40	33		
Cu	20	15		
Nb	17	17		
O	7	6		
P	<50	–		
B	<10	–		
Mo	<10	–		
Sn	<50	–		
As	<50	–		
Os	–	3240	1.54	1.41
Pt	–	2300	1.73	1.52
Re	–	256	3.6	1.48
Ir	–	216	3.8	1.43
H	–	57 385	–	–
He	–	9241	–	–
Fe	889 600	757 340	0.25	1.19

generally no – or virtually no – driving stress acting on the dislocation line of the loop [11]. [1] According to Eq. (6) the activation energy $E_M \to \infty$ as $\tau \to 0$, but this is for infinitely long dislocation lines which allow $X \to \infty$. In our case the lines are of finite length, i.e. $X = nb$, with typically $n \approx 25$. Thus, for the loop, from Eq. (4),

$$E_M(n) \approx E_L \left(\frac{nb}{\xi_L} \right)^{1/3}. \tag{8}$$

3.2. Numerical examples

For a numerical example we shall apply the above to a typical reduced-activation ferritic martensitic steel alloy (EUROFER 97), favoured as a candidate for the first wall of a fusion power plant. We assume the alloy to have been irradiated with a neutron first wall power load of 4.15 MW m^{-2}, for a service time of 10^4 days (≈27 years), corresponding to a fluence of 1.6×10^{28} nm^{-2}. The composition, both original and after irradiation, is given in Table 1. The three principal substitutional alloy elements, in atomic percentage after irradiation, are Cr 9.4, W 0.57 and Mn 5.56. Most of this Mn (i.e. 5) is produced by transmutation, but the other elements are less varied from their original contents (Cr 9.0, W 1.08). Of the other atoms, only H (5.7) and He (0.9) are produced in significant amounts, but we shall not consider these, here, because, being interstitial and highly mobile, they are unlikely to remain in simple solid solution. Hence we consider only the Cr, W and Mn in solid solution interaction with a loop.

For the binding energy of such an atom in the core of an edge dislocation, we use the standard expression [12] for the elastic interaction

[1] However, in the inhomogeneous elastic field of a long grown-in dislocation line, this stress may act more strongly on one side of a loop than oppositely, on the other side; and so drive the loop forwards or backwards. There is, in fact, evidence for the clustering of loops round grown-in dislocations [11].

$$U_0 = 4\mu r_0^3|\eta|, \tag{9}$$

where $r_0(\approx b/2)$ is the atomic radius of the host atom and η is the misfit factor,

$$\eta = \frac{r_s - r_0}{r_0}, \tag{10}$$

for a solute atom of radius r_s. This expression for U_0 is of course approximate but comparison with measured values for copper-based alloys [12] has shown it to be reasonably reliable. Values are given in Table 2.

In Table 2, the value $Tb \approx 1$ eV is smaller than the conventional one, $Tb \approx \frac{1}{2}\mu b^3$ (≈ 4 eV for Fe). However, the latter applies to the case where the 'wavelength' of the dislocation curve, i.e. the range R of the extra elastic field due to this, in the standard expression

$$T = \frac{\mu b^2}{4\pi} \ln\left(\frac{R}{b}\right), \tag{11}$$

is large, e.g. $R \approx 500b$, whereas the present dislocation loops are small, e.g. $R \approx 5b$.

Table 2 shows that the average spacing of W atoms along the dislocation line is about $10\xi_L$. It follows that the flexibility of the line, on this scale, is sufficient to allow each W atom obstacle to be individually activated, with no cooperative effects from others. In this case, as noted above, the activation energy is simply U_0 i.e. ≈0.4 eV, at each W atomic obstacle. The situation with Mn is marginal, since the average spacing is about $1.2\xi_L$, but the line flexibility is likely to make this case more similar to that of W than that of the continuum hills and valleys. Hence we assume a one-atom obstacle also, for Mn, with $U_0 \approx 0.3$ eV.

In these examples the size of the dislocation loop plays only a secondary role in that, the larger the loop, the more places there are along it for one-atom obstacles which have to be overcome by thermal activation before the loop can move forward as a whole.

Table 2
Parameters for the interaction of substitutional solute atoms with a dislocation loop in irradiated EUROFER 97 alloy

Parameter	Cr	Mn	W
Atomic concentration (cb^3)	0.094	0.056	0.0057
Radius of solute atom [17] r_s (nm)	0.125	0.133	0.137
$\|\eta\|$ (Eq. (10), with $r_0 = 0.124$ mm for Fe)	0.008	0.072	0.105
U_0 (eV) in Eq. (9)	0.032	0.29	0.42
ξ_L/b ($Tb \approx 1$ eV)	13	3.7	5.1
N (Eq. (7))	4.9	0.83	0.11
Activation energy, Q (eV)	0.04	0.3	0.4
$\exp(-Q/kT)$ at 300 K	0.15	6×10^{-6}	10^{-7}
$\exp(-Q/kT)$ at 1000 K	0.57	0.027	0.008

The example of Cr is quite different. Here there are about 5 Cr atoms in the length ξ_L, and still more in a typically sized loop, so that the hills and valleys model is now more appropriate. The values in Table 2 give, from Eq. (2), $E_L = 0.038$ eV for Cr. Eq. (4) requires a value for X, which we take to be the length of the dislocation loop. The typical value, $25b$, for this then gives $E(X) \approx 0.038 \times 1.24$ and so $Q = 0.047$ eV in Table 2.

Each value of $\exp(-Q/kT)$ in the table represents an 'immobilization factor' in the sense that, if a loop jumps from one lattice position to the next with frequency v in the pure metal, then it does so with reduced frequency $v\exp(-Q/kT)$ in the alloy.

At 300 K the immobilization of the loop by W atoms is most severe, despite the low concentration of this solute, and this is a result of its misfit η. Although Mn is almost 10 times more abundant, in the irradiated alloy, this does not compensate for its relative ineffectiveness, compared with W. Because of its very small misfit, Cr makes a negligible contribution.

At 1000 K, the differences are much less extreme, although the contribution of Cr is still small. W still gives the most extreme immobilization factor, but this is no longer sufficient to overwhelm the effect of the greater abundance of Mn, which now provides the greatest obstruction to the movement of the loop. At 1000 K, a single W atom and six Mn atoms, for example, on a loop exert roughly comparable obstructions. We thus define a single effective activation energy for each of these seven obstacles, using Labusch's expression [13], based on the argument that the dislocation speed is determined by the reciprocal of the sum of waiting times with different activation energies,

$$U_{\text{eff}} = \frac{\sum_i U_i \exp\left[\frac{U_i}{kT}\right]}{\sum_i \exp\left[\frac{U_i}{kT}\right]}, \tag{12}$$

for obstacles i, which gives $Q_{\text{eff}} = U_{\text{eff}} = 0.337$ eV and thus $\exp(-Q_{\text{eff}}/kT) = 0.0175$. Each of these seven averaged obstacles is less severe than that of a single W atom (0.008), but an individual activation now moves only a short (≈25/7 atoms) length of the loop, whereas in the single W atom case, the entire loop is free to move once this one obstacle is overcome.

As a second example we consider the results of Ehrhart and Averback [6] on Ni, $NiSi_{0.01}$ and $NiGe_{0.01}$, after neutron irradiation at 6 K. After annealing at 300 K the pure Ni showed a fairly even distribution of SIA loops with radii from 0.5 to 2 nm, whereas the $NiSi_{0.01}$ alloy showed very few loops with radii above 1 nm. The $NiGe_{0.01}$ alloy showed an intermediate behaviour. Because 300 K is below the temperature (480 K) at which vacancies become mobile, the coarser structure in the

pure Ni is evidently due to the mobility of the small (0.5–1 nm) loops and this is absent in the alloy, a difference which the authors attribute to pinning of loops by the solute atoms. The atomic concentration 0.01 implies that there was on average only one solute atom in interaction with the dislocation core of a loop, assuming this latter to have a length $\approx 25b$. The misfit factor, 0.056 (Si), 0.016 (Ge), gives $\xi_L \approx 8b$ (Si), $19b$ (Ge). Hence conditions are such that, as for W in the previous example, single solute atom activation occurs, with activation energy $U_0 = Q$, giving, at 300 K, $\exp(-Q/kT) = 2 \times 10^{-4}$ (Si), 0.09 (Ge). The Si is thus expected to immobilize the loops severely, and the Ge mildly, at this temperature. At 480 K, these values are modified to 5×10^{-3} (Si), 0.2 (Ge) but the effect of this weakened immobilization is over-ridden by the vacancy mobility at this temperature, which profoundly modifies the microstructure.

4. Conclusion

When SIA clusters have the form of edge dislocation loops, the immobilizing effect of randomly distributed substitutional solute atoms is an example of solid solution hardening. However, features of these loops make the immobilization different in some respects from standard solid solution hardening. In particular, the finite, short, length of the loop dislocation line necessitates that the activation energy to unpin the loop remains finite even without applied stress to drive the loop. The interaction of such a solute with a loop becomes significant only when the solute atom sits in the central core of the edge dislocation. It is assumed that this interaction is elastic. Other interactions (electrical, chemical) are small by comparison, for the solutes considered here [14].

Because a loop is short, e.g. 25 atoms long, the number of solute atoms on it in a dilute solution, e.g. 1 at.%, is too small for the continuum representation of the standard solid solution hardening theory. The immobilizing effects of single solute atoms then have to be considered individually. The continuum model becomes more useable for concentrations greater than about 10%. The elastic interaction stems from the size misfit of the solute atom and the results show a sensitive dependence of immobilization on misfit, particularly at room temperature, but less so at expected fusion power plant operating temperatures.

Applied to an iron-based alloy (EUROFER 97) favoured for a fusion power plant, after 10^4 days service in which 14 MeV neutron irradiation produces transmutations, the results show that the most significant solutes are Cr, W and Mn. Although much the most abundant, Cr is a weak immobilizer because of its small size misfit. Despite its low concentration, W, with a large misfit, is the most potent immobilizer. In general, because transmutations of the Fe host atoms produce other transition metals of similar atomic sizes, the effects of transmutations are minor. The exception to this is Mn, both because it is produced by transmutation in some abundance and also because it has a fairly large misfit in Fe. As a result, the immobilizing effect of transmutation Mn is strong, even though outmatched by that of the initial W alloy atoms.

Acknowledgements

It is a pleasure to thank Ian Cook for encouragement and stimulating discussions and M. Zaiser for helpful comments.

Appendix A

A.1. Calculations

A popular low-activation ferritic martensitic structural steel was used [15] as a basis for this calculation: EUROFER 97. The atomic constitution experimentally measured for a set of heat sample data was here averaged to give a typical base composition of the unirradiated material C_i where i refers to a constituent chemical element. These data are given in Table 1.

The transmutation data were taken from the European Activation System (EASY) database [16] and relate to the conceptual tokamak power plant EEF for conditions pertaining to the outboard first wall (zone 12), blanket and shield positions. We calculate transmutations in this zone, assuming the alloy to have been irradiated with a neutron first wall power load of 4.15 $\mathrm{MW\,m^{-2}}$, for a service time of 10^4 days ($\approx$27 years), corresponding to a fluence of 1.6×10^{28} $\mathrm{nm^{-2}}$. The concentrations, $C_{i,j}^{\mathrm{Trans}}$, of the transmutation products (i.e. the jth transmutant species arising from the ith base constituent element) were calculated after an assumed irradiation time of 10^4 days ($\approx$27 years). This time is approximately the required economic lifetime of the power plant but is longer than the proposed blanket replacement time, currently considered to be $\approx$5 years. To deduce the concentrations for other irradiation times, the results scale approximately in linear proportion with the ones given here. The calculated impurity concentrations, C_j^{Trans}, are given by the summation over all transmutation branches

$$C_j^{\mathrm{Trans}} = \sum_i C_i C_{i,j}^{\mathrm{Trans}}. \tag{A.1}$$

Secondary transmutation branches (i.e. transmutations of transmutations) were not considered here.

Table 3
Measured densities and mean distances between various defects after mixed proton and neutron irradiation of F82H ferritic-martensitic steel (<12 dpa) [18]

Defect type	Density (m^{-3})	Mean separation, L (nm)
Defect SIA loops/clusters	4×10^{22}	30
Dislocations	$<5\times10^{14}$	45
'Nano voids' (diameter $\simeq$1 nm)	5×10^{23}	12

A.2. Results

Results are given in Table 1, column 3. Transmutation species having concentrations below 100 appm are not listed in the table but these low concentration elements are: Sc, Si, S, Al, Mg, Cl, Na, Ne, Ca, Li, Be, N, B, Hg, Hf, Ta, Ar, K, Mo, Zr, Y, Ru, Tc, Sr, Nb, Rh, Cu, Pd, Zn, F, O, P, Te, Sb, Cd, In, I, Xe, Se, Ge, Ga, Br, Kr.

In Table 1 we assume a uniform distribution of all substitutional alloy atoms, including transmuted ones, to estimate the mean separation, $\langle d\rangle$, between foreign atoms and compare this distance with the mean separation, $\langle L\rangle$, between known and measured defects of other types in irradiated material (Table 3). It can be seen that the various values of $\langle d\rangle$, listed in Table 1, are all smaller than the values of L (Table 3); thus the foreign atoms are expected to have an important effect on the SIA loops.

The atomic volumes of the foreign atoms are also given in Table 1. They serve to guide thinking about which atoms give the largest misfits and immobilization of the SIA loops.

References

[1] A.J.E. Foreman, C.A. English, W.J. Phythian, Philos. Mag. A66 (1992) 655.
[2] M. Kiritani, J. Nucl. Mater. 251 (1997) 237.
[3] T. Hyashi, K. Fukumoto, H. Matsui, J. Nucl. Mater. 307–311 (2002) 930.
[4] T. Hyashi, K. Fukumoto, H. Matsui, J. Nucl. Mater. 307–311 (2002) 951.
[5] T. Hyashi, K. Fukumoto, H. Matsui, J. Nucl. Mater. 307–311 (2002) 993.
[6] P. Ehrhart, R.S. Averback, Philos. Mag. A60 (1989) 283.
[7] A.V. Barashev, Yu.N. Osetsky, D.J. Bacon, Philos. Mag. A80 (2000) 2709;
Y.N. Osetsky, D.J. Bacon, A. Serra, B.N. Singh, S.I. Golubov, Philos. Mag. 83 (2003) 61.
[8] D.G. Martin, Philos. Mag. 7 (77) (1962) 803.
[9] M. Zaiser, Philos. Mag. A82 (2002) 2869.
[10] A.I. Larkin, Sov. Phys. JETP 31 (1970) 784;
R. Labusch et al., in: Rate Processes in Plastic Deformation, 26, American Society for Metals, Metals Park, OH, 1975.
[11] B.N. Singh, N.M. Ghoniem, H. Trinkhaus, J. Nucl. Mater. 307–311 (2002) 159.
[12] N.F. Fiore, C.L. Bauer, in: B. Chalmers, W. Hume-Rothery (Eds.), Progress in Materials Science, 13, Pergamon, Oxford, 1967.
[13] R. Labusch, Czech. J. Phys. B38 (1988) 474.
[14] P. Haasen, in: F.R.N. Nabarro (Ed.), Dislocations in Solids – 4, North-Holland, Amsterdam, 1979, p.155.
[15] R. Lindau, (2001) private communication.
[16] C.B.A. Forty, R.A. Forrest, D.J. Compton, C. Rayner, AEA Technology, reports AEA FUS 180 (1992) and AEA FUS 232 (1993).
[17] W.B. Pearson, Handbook of Lattice Spacings, Pergamon, New York and London, 1958.
[18] X. Jia, Y. Dai, M. Victoria, J. Nucl. Mater. 305 (2002) 1.